THE JOURNAL OF PHYSICAL CHEMISTRY A

Article

Structures and Electronic Properties of TiV (N=1-16) Clusters: First-Principles Calculations

Peter Ludwig Rodríguez-Kessler, and Adán Rubén Rodríguez-Domínguez

J. Phys. Chem. A, **Just Accepted Manuscript** • DOI: 10.1021/acs.jpca.6b00224 • Publication Date (Web): 04 Apr 2016

Structures and Electronic Properties of Ti_nV (n=1-16) Clusters: First-Principles Calculations

P. L. Rodríguez-Kessler[†] and A. R. Rodríguez-Domínguez[*,‡]

Instituto Potosino de Investigación Científica y Tecnológica, San Luis Potosí 78216, México, and Instituto de Física, Universidad Autónoma de San Luis Potosí, 78000, México

E-mail: adnrdz@ifisica.uaslp.mx

[*]To whom correspondence should be addressed
[†]Instituto Potosino de Investigación Científica y Tecnológica, San Luis Potosí 78216, México
[‡]Instituto de Física, Universidad Autónoma de San Luis Potosí, 78000, México

Abstract

Structures and electronic properties of Ti_nV ($n = 1 - 16$) clusters have been investigated using density functional theory (DFT) with the generalized gradient approximation (GGA). The calculations have shown that the Ti_nV clusters favor compact spherical structures having similar conformations to the pure Ti_n clusters. The results show that the vanadium atom remains on the surface when $n \leqslant 8$ and $n = 16$, while for $n = 9 - 15$, it occupies the endohedral position. The Ti_6V, $Ti_{12}V$, and $Ti_{14}V$ clusters are found to be more stable than their neighbors, consistent with pure Ti_n clusters that have the same size. Additionally Ti_4V has been found to be also magic, consisted with recent reports of B and Al-doped Ti clusters. Small Ti_nV ($n \leqslant 4$) clusters exhibit a transition from metallic-like to semi-metallic electronic structure, while for $n = 5$ onwards, no significant changes are observed compared to pure Ti_n clusters.

Keywords

TiV clusters, Titanium, Density functional theory, DFT

Introduction

Subnanometer clusters are considered a new phase of matter, being the bridge between atoms and the bulk. They form part of an extensive research due to various potential applications.[1,2] It has been found that atomic clusters for a wide type of elements are suitable to undertake catalytic reactions including gold, which is practically inert in the bulk, and the capability of gold to be reactive is one of its most attractive properties.[3,4] There is considerable interest in the structures and properties of subnanometer clusters for example for their use as finely divided metal catalysts, particularly for bimetallic clusters, which offer the opportunity of tuning their activity and selectivity. To date, much work has concentrated on small clusters of late transition metals e.g. noble and platinum metals, while little has been

done for the early transition metals. Among transition metal (TM) clusters, the reactivity of titanium clusters is not fully understood, due to the complexity of the almost empty d band which provide unique bonding properties.[5] Recently, a number of studies of titanium clusters were focused in studying the physical and electronic properties. Early experiments on Ti_2 clusters by[6–9] revealed that the binding energy varies from 2.1 to 1.05 eV, which was considered as the lowest limit by Haslett et al.[7] In 1980, C. Cossé et al. determined the Raman spectrum of the isolated Ti_2 dimer.[10] Sakurai et al.[11] determined that $N = 7$, 13, 15, 19 and 25 are magic numbers of titanium clusters. Wu et al.[12] performed anion photoelectron spectroscopy experiment for Ti_n clusters with $n = 2 - 65$. Theoretically, Wei et al.[13] studied Ti clusters up to $n = 10$ using density functional theory (DFT) and came to the conclusion that the electronic structures of the titanium clusters develop some bulk-like features at rather small size. Zhao et al.[14] studied the structures and electronic properties of Ti_n clusters ($n = 2 - 14$, 19, 55) by the plane wave ultrasoft pseudopotential method suggesting that Ti clusters favor a pentagonal growth pattern. Villanueva et al.[15] studied Ti_n clusters from $n = 2 - 15$ using DFT with the Lee-Yang-Parr (LYP) functional and found that Ti_7 and Ti_{13} clusters show higher stability than other clusters, which has been confirmed with experiments. Ascencio et al.,[15] identified three magic number clusters Ti_7, Ti_{13} and Ti_{15}, corresponding to closed-packed structures. In spite of the number of works based on Ti clusters, a few studies on doped Ti clusters were carried out in both experiment and theory. This may be due to the existence of d electrons, since the size-dependent variations cannot be explained by the shell models of s valence electrons.[16] Recent studies showed that the chemical and electronic properties of titanium clusters could be tuned by doping. In particular, doped titanium clusters with formula $Ti_{12}M$ have shown higher stability when the dopant M turns out to be placed at the center of the cage, which can be understood from the pseudo-spherical icosahedral structure, which has been observed with a high stability for other metallic clusters. Xiang et al.[17] studied Al-doped Ti_n clusters using density functional theory and found that the Al remains on the surface of the clusters for $n < 9$, while it occupies

the center of the cage for $n = 9$ onwards. J. Du et al.[18] studied B-doped Ti_n clusters and found that the isomers with a B atom located on the surface are energetically favored for most of the studied clusters except $Ti_{12}B$. Furthermore, J. Du et al. demonstrated that the electron transfers from Ti atoms to the impurity contributes for the stability of Small M-doped Ti_{1-4} clusters ($M = V, Fe, Ni$),[19] however, as far as we know, the structures and electronic properties of larger Ti_nV clusters (that have $n > 4$) are not investigated until now. In this work, we studied the growth behaviour of Ti_nV ($n = 1-16$) clusters and found that the $Ti_{n-1}V$ clusters hold similar structural conformations than the bare Ti_n clusters. It turns out that the V impurity remains on the surface when $n \leqslant 8$ and $n = 16$, while for $n = 9-15$, it occupies the cage center. The analysis of the binding energy indicates that the Ti-V bond strength increase for clusters with $n = 11-13$ atoms, especially for $Ti_{12}V$, which adopts the icosahedral geometry. The electronic structures of small Ti_nV ($n \leqslant 4$) clusters exhibit a transition from metallic-like to semi-metallic electronic structure, while for $n = 5$ onwards, no significant changes are observed compared to pure Ti_n clusters.

Computational Details

In metal clusters all their physical and chemical properties depend on its structure, and their determination is one of the most fundamental and important tasks. The determination of the most stable structure requires finding the global minimum of the potential energy surface (PES), which gives the energy of a system as a function of its atomic coordinates.[20] For this task, almost all algorithms require an enormous number of evaluation of PES, thus a systematic search for the global minimun is necessary. Various levels of theory have been used with the aim of predicting the structure of TM clusters. Empirical potentials are not always reliable for structure prediction because they typically neglect the directional nature of $d-d$ interactions and quantum effects such as those arising from spin magnetism, orbital symmetry, and electronic shell closings.[21] It is because of this that we use the *ab initio* method to

describe the partially filled d shells and strong electron correlation. For the evaluation of PES a set of initial structures are obtained using graph theory with the methodology described in our previous work,[22] which allows us to explore the configuration space for small clusters ($n \leqslant 7$). We systematically generate the Ti_nV alloy structures for a given cluster size by replacing the V impurity in all Ti positions of the initial structures. For each size, the center of mass and number of Ti-V, and homogeneous Ti-Ti bonds is compared. This procedure allow us to reduce the number of isomorphic structures. All the resulting structures are optimized by *ab initio* calculations. From $n = 8$ onwards, the structures of Ti_nV clusters are constructed based on those of smaller doped clusters by adding a single atom on all inequivalent binding sites on the surface of the equilibrium structures of $Ti_{n-1}V$ clusters. This procedure however, generates a large number of structures, increasing the computational complexity, because of this, we only decorate stable clusters whose relative energy is less than $\Delta E = 1$ eV from the ground state. The principle of this procedure is that the clusters follow a growth pattern from the preceding ones. The calculations in this work are based on the framework of spin-polarized density functional theory (DFT)[23,24] implemented in the code Vienna *ab initio* simulation package (VASP),[25,26] which solves the Kohn-Sham equations under periodic conditions with a plane wave basis set. The interactions between the ions and valence electrons are described by the projector augmented-wave (PAW) method.[27] The exchange correlation (XC) functional is treated using the PBE approximation.[28] The wave functions are expanded in plane-wave basis sets with a cutoff energy of 400 eV. The atomic positions are relaxed self-consistently by the conjugate gradient method algorithm until the forces are smaller than 0.01 eV/Å for all atoms. We used a supercell with a distance of 10 Å of vacuum between periodic images, which is large enough to avoid their interaction. Due to the size of the supercell, only the Γ point is taken into account to represent the Brillouin zone. For the finding of the global minimum PES of Ti_nV clusters, for each structure multiple spin states are considered. For each cluster size, the local minima of the potential energy surface on the lowest energy configuration is proven by the harmonic vibrational frequencies. To check

the accuracy of our calculation, the binding energy and bond length of Ti_2 and TiV dimers are compared with theoretical and experimental values as shown in Table 1. Additionally, for the calculation of the anionic state, a background charge was applied to maintain charge neutrality. The dipole and quadrupole moment corrections were taken into account[29] to properly screen out long range Coulomb interactions.

Table 1: Calculated equilibrium bond length and binding energy for Ti_2, and TiV dimers in the ground state configuration.

Dimer	Method	Functional	Bond length (Å)	Binding energy (eV/at.)
Ti_2	PAW [a]	PW91	1.92	1.61
	all-electron [b]	PW91	1.958	2.57
	This work	PBE	1.897	1.875
	US PP [c]	GGA (PW)	1.92	2.34
	Expt. 1 [d]		1.943	-
	Expt. 2 [e]		-	1.54 ± 0.19
TiV	This work	PBE	1.788	1.875
	LCAO [f]	BPBE	1.838	2.27

[a] Ref. [30]
[b] Ref. [18]
[c] Ref. [14]
[d] Ref. [31]
[e] Ref. [32]
[f] Ref. [19]

Results and discussion

The equilibrium structures of the pure Ti_n clusters that have $n = 2 - 17$ are optimized on the basis of previous calculation results. Anderson[33] concluded that titanium clusters have tightly packed structures by using the molecular orbital method, which is in good agreement with our result. Our calculation shows that the most stable structure of Ti_3 is an equilateral triangle with D_{3h} symmetry. The stable structures of Ti_{4-6} are an axially distorted tetrahedron with C_{3v} symmetry, a distorted trigonal bipyramid (TBP) structure with C_{2v} symmetry, and a C_{2v} octahedron, respectively. In accordance to Wei et al. these clusters have not regular symmetries like a regular tetrahedron (T_d) trigonal bipyramid (D_{3h}) and octahedron (O_h). In contrast, for Ti_6, J. Du et al. found a C_{2v} structure with 4 μ_B

as the ground state. Ti_7 is a pentagonal bypidamid (PBP) structure with a singlet state. For Ti_8, a bicapped octahedron with D_{2d} symmetry is the most stable structure. For Ti_9 to Ti_{12} clusters, the ground state is formed by a partial icosahedron structure. The ground state of Ti_{13} is formed by a Jahn-Teller distorted icosahedral structure with 6 μ_B, while the most stable structure of Ti_{15} is a bicapped hexagonal antiprism with 4 μ_B of total magnetic moment. Ti_{14} is a capped icosahedron. For $n = 16$ and 17, we found a closed-packed structure for the Ti_n clusters, which is expected due to the delocalization of $3d$ electrons. In order to determine the effect of the V impurity, we used the results of the bare Ti_n clusters as reference systems. As far as we know, the structures of V-doped Ti_n (with $n > 4$) clusters are not investigated so far, it is because of this that we have performed an extensive search to find the minimum energy structure described in the previous section.

Table 2: Ground-state structures and low-lying isomers of Ti_n and $Ti_{n-1}V$ ($n = 3-6$) clusters. For each cluster the total magnetic moment (in μ_B), and the binding energy (eV) is given. The gray and dark spheres represent Ti and V atom, respectively.

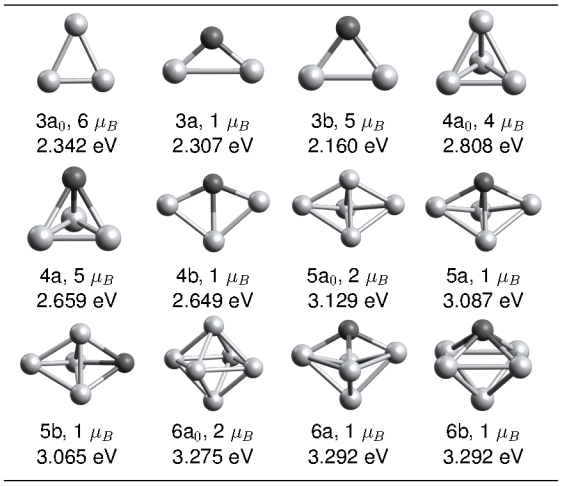

The lowest energy structures and some metastable low-energy isomers (from Ti_2V to Ti_5V) are presented in Table 2, including their Ti_n cluster counterpart for comparison. Each structure is labeled with a number and a letter corresponding to the total number of atoms, and the alphabetic order is attached to the isomers in descending order of cluster stability.

The structures of pure Ti_n are also included in Table 2 as well as the binding energy per atom (E_b), and total magnetic moment (μ). The ground state structure of the TiV dimer is a triplet state with a binding energy of 1.87 eV/atom and Ti-V bond length of 1.78 Å shorter than that of the Ti_2 dimer, with 1.89 Å. Using the BPBE functional, J.G. Du et al.[19] obtained a bond distance of 1.838 Å for the TiV dimer, which is in close agreement with our result. They found a dissociation energy of 2.27 eV/atom, which is slightly larger than the calculated in the present work. The Bader charge analysis indicates that a charge transfer occurs from the Ti atoms to the V impurity, consistent with Ref. 19. This behaviour may derive from the larger electronegativity of V (1.63), with respect to Ti atom (1.54). The ground state structure of Ti_2V is an open triangle with 98.4° for the $\angle$ Ti-V-Ti angle and with Ti-V distances of about 1.83 Å. The magnetic moment is 1 μ_B, which is significantly lower than Ti_3 with 6 μ_B. For the Ti_3V cluster the most stable structure is a tetrahedron with 5 μ_B, while a planar rhombus with 1 μ_B is only 0.04 eV higher in energy. Ti_4V and Ti_5V clusters are formed by a TBP and an irregular octahedron (O_H) structure, respectively. Notice that from Ti_2V to Ti_5V clusters, the doped clusters have the same conformation than the bare Ti clusters where the V impurity occupies the top site. The ground-state geometries and isomers of clusters (from Ti_6V to $Ti_{11}V$) are shown in Table 3. In the case of Ti_6V, the most stable structure (7a) is a PBP, in which the V atom occupies the most coordinated position, which is 0.09 eV more stable than the 7b isomer, in which the V impurity is located in the vertex site. A bicapped octahedron is obtained for Ti_7V as the lowest energy structure, where the V atom occupies the surface site. For Ti_8V, a bicapped PBP is the most stable structure. The most stable structures of $Ti_{9-11}V$ clusters have an icosahedral growth, where the V impurity is trapped on the center of the cluster conserving the shape of the host cluster, except for $Ti_{10}V$ in which the structure is slightly distorted.

The ground-state geometries and isomers of clusters (from $Ti_{12}V$ to $Ti_{16}V$) are shown in Table 4. The most stable structure of $Ti_{12}V$ can be considered as a distorted icosahedral structure, but not a regular icosahedron (I_h) in which the impurity is located in the center of

Table 3: Ground-state structures and low-lying isomers of Ti_n and $Ti_{n-1}V$ ($n = 7-12$) clusters. For each cluster the total magnetic moment (in μ_B), and the binding energy (eV) is given. The gray and dark spheres represent Ti and V atom, respectively.

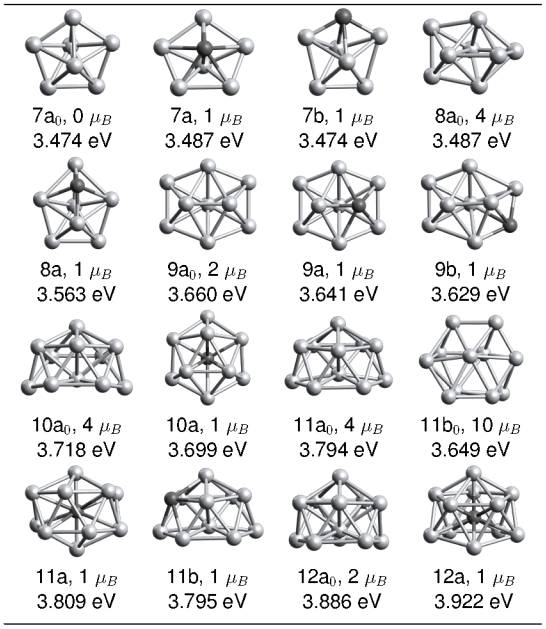

the cage. This feature has been observed for $Ti_{12}M$ clusters when doped with M=B and Al, while for the other sized clusters, the impurity usually adopts the surface site. The $Ti_{12}V$ isomer in which the V atom occupies the surface site is about 0.83 eV higher in energy. In $Ti_{13-15}V$ clusters the V impurity is also trapped in the center of the cluster. Nevertheless, for $Ti_{16}V$, which is the largest cluster considered in this work, the V impurity occupies the surface site. It is interesting to note that the structures of the Ti_nV clusters can be obtained by adding an impurity atom on the most stable Ti_n clusters.

Electronic structure

The stability of Ti_n and Ti_nV clusters is investigated by calculating the binding energy per atom (E_b), second order energy differences (Δ_2E), and dissociation energy (E_d), defined as

Table 4: Ground-state structures and low-lying isomers of Ti_n and $Ti_{n-1}V$ ($n = 13-17$) clusters. For each cluster the total magnetic moment (in μ_B), and the binding energy (eV) is given. The gray and dark spheres represent Ti and V atom, respectively.

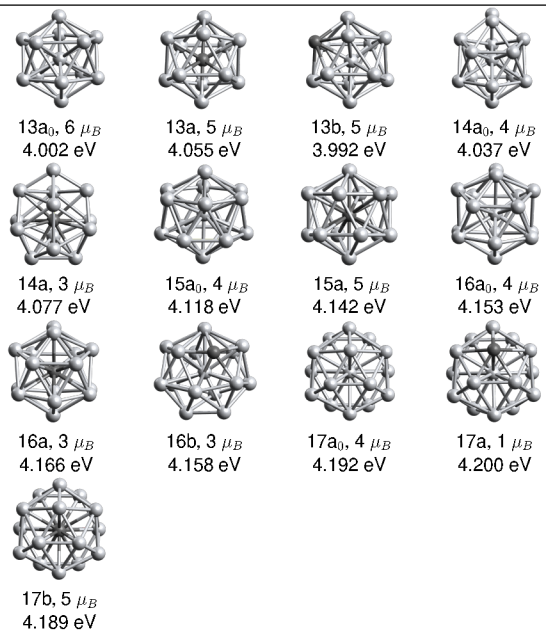

$$E_b[Ti_n] = [nE_T(Ti) - E_T(Ti_n)]/n, \qquad (n = 2, 3, ..., 17) \tag{1}$$

$$\Delta_2\mathrm{E}[Ti_n] = E_T[Ti_{n+1}] + E_T[Ti_{n-1}] - 2E_T[Ti_n], \tag{2}$$

$$\mathrm{E_d}[Ti_n] = E_T[Ti_{n-1}] + E_T[Ti] - E_T[Ti_n], \tag{3}$$

for the pure Ti_n clusters, and

$$E_b[Ti_nV] = (nE_T[Ti] + E_T[V] - E_T[Ti_nV])/(n+1), \qquad (n = 1, 2, ..., 16) \tag{4}$$

$$\Delta_2\mathrm{E}[Ti_nV] = E_T[Ti_{n+1}V] + E_T[Ti_{n-1}V] - 2E_T[Ti_nV], \tag{5}$$

$$\mathrm{E_d}[Ti_nV] = E_T[Ti_{n-1}V] + E_T[Ti] - E_T[Ti_nV], \tag{6}$$

for the V-doped Ti_n clusters, where $E_T[Ti]$, $E_T[V]$, and $E_T[Ti_nV]$ are the total energies of the bare Ti atom, the V atom, the Ti_nV doped cluster, while n denotes the number of Ti atoms in the cluster, respectively. The Figure 1 shows the binding energy of pure Ti_n and $Ti_{n-1}V$ clusters for $n = 2 - 17$. For the bare Ti_n clusters, E_b gradually increases with the cluster size n rapidly up to $n \leqslant 7$ and then the size dependence become smooth at $n > 7$. When Ti clusters are doped with V, the binding energy is similar for $Ti_{1-10}V$ clusters, except for Ti_3V and Ti_6V clusters, where it is lower than for pure Ti_n clusters. Interestingly, for $Ti_{12}V$ and its first neighbors, the binding energy is slightly larger, while for $n = 15$ onwards the Ti clusters become more stable. The increased stability of the $Ti_{12}V$ cluster can be understood by the icosahedral structure of $Ti_{12}V$. The high stability of the regular icosahedral structure usually occur for transition metal clusters. In a recent paper by us, we found that the icosahedral structure has a special reactivity when compared with less coordinated structures.[22]

The second order energy difference $\Delta_2 E$ and dissociation energy E_d help us to determine the relative stability of Ti_nV clusters compared with their neighbors. For $\Delta_2 E$ and E_d (see Figures 2a and 2b), an odd-even pattern is shown with the maximum values at $Ti_{12}V$ followed by $Ti_{14}V$, Ti_6V, and possibly Ti_4V clusters. Those sizes correspond to the magic numbers of Ti_6, Ti_{13} and Ti_{15} clusters, in excellent agreement with previous theoretical and experimental results. Interestingly, J. Xiang et al. found that Ti_4Al is also magic, which supports our finding for the Ti_4V cluster. As in Eq. 6, we calculated the V dissociation energy E_d[V] as shown in Figure 2c, and found similar energy variation than for the Ti dissociation energy.

It is very interesting to mention that anionic Ti_n^- and neutral Ti_nV clusters are isoelectronic but differ in one component atom. To compare the differences between them, we calculated the anionic Ti_n^- clusters based on the structure isomers of the neutral Ti_n and Ti_nV clusters considering five spin multiplicities. Additionally, we calculated the electron

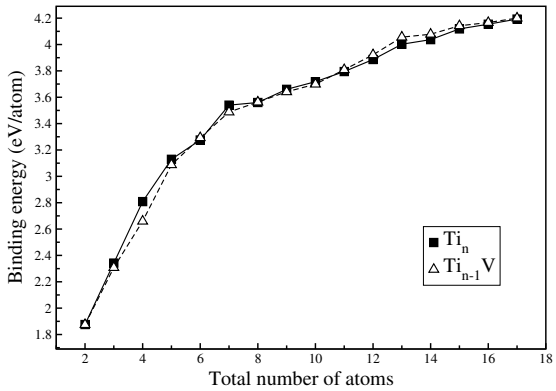

Figure 1: Comparison of the binding energies of Ti_n and $Ti_{n-1}V$ clusters. Note that we are comparing clusters with the same size, (e.g. for $n = 6$, Ti_6 and Ti_5V lie at the same value).

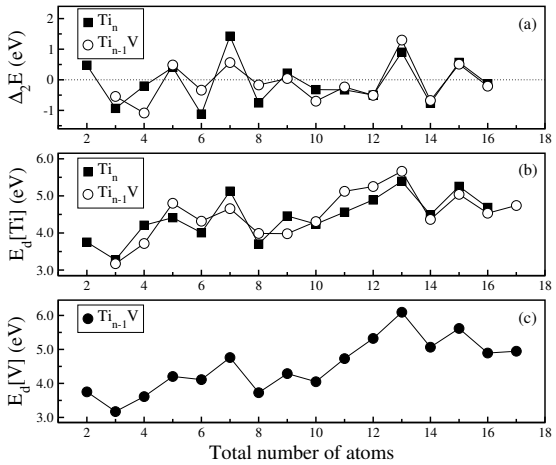

Figure 2: (a) Comparison of the second difference of the most stable Ti clusters as a function of n, (b) Ti dissociation energy E_d[Ti] for Ti_n (Eq. 3) and $Ti_{n-1}V$ (Eq. 6) and (c) V dissociation energy E_d[V] for $Ti_{n-1}V$ as a function of the cluster size n.

affinity (EA), which is an important quantity to characterize metal clusters, defined as

$$EA_n = E_T(Ti_n) - E_T(Ti_n^-), \tag{7}$$

where $E_T(Ti_n)$ and $E_T(Ti_n^-)$ are the total energies of the neutral Ti_n and anionic Ti_n^- clusters. In Figure 3a we show EA_n of Ti_n^- clusters as a function of size. We found smaller values than the experimental reported ones, but closer than a recent DFT calculation by Kummar et al.[5] EA_n increases gradually with the size with a minimum at $n = 7$, in agreement with the experimental data.[34] We found that Ti_n^- clusters favor the structures of the neutral Ti_n clusters rather than that of the V doped Ti_n ones. In Figure 3 we also show the calculated second order energy differences of Ti_n^- clusters and found that their stability is more sensitive to the size than that of the neutral Ti_nV ones (as shown in Figure 2a).

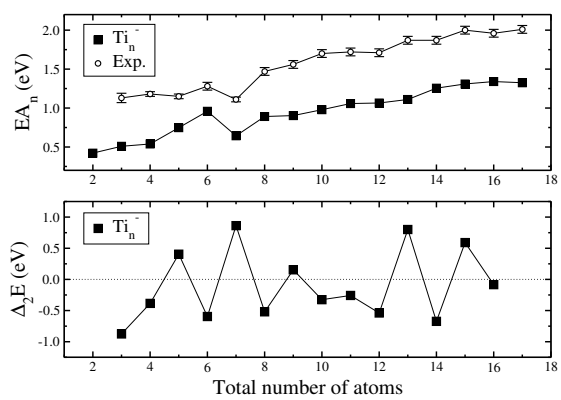

Figure 3: The EA_n (top) and $\Delta_2 E$ (bottom) of the most stable anionic Ti_n^- clusters is presented.

In order to have some insight into bonding nature, we show the Ti-V and Ti-Ti average bond lengths (ABL) of Ti_nV clusters are shown in Figures 4a and 4b. The Ti-V bond length gradually increases from Ti_3V to $Ti_{15}V$ clusters, and exhibits two minima at Ti_6V and $Ti_{12}V$, and possibly $Ti_{16}V$, on the curve. Those sizes correspond to Ti_nV clusters that have stronger Ti-V bonds but less pronounced Ti-Ti bonds, indicating that these structures may have more delocalized V-Ti bonds. To prove that, we calculated the total density of

states (DOS) of the Ti_nV clusters with the addition of the local density of states (LDOS) of the V impurity as shown in Figure 5. For simplicity, we present the DOS calculation without spin-polarization corresponding to the non-magnetic state. From the present DOS curve, we can observe that from Ti_1V to Ti_4V clusters, the total DOS have a molecule-like energy distribution with a number of localized peak features. That is to say, the V impurity affects the metallic behaviour of small Ti_n clusters. From Ti_5V onwards, and overlap between the energy levels leads to a continuous energy band which eventually continues to the bulk as the size increases. $Ti_{12}V$ is a special case, in which a high peak is located at the Fermi level, giving us an insight of the high reactivity of the icosahedral cluster. Interestingly, the DOS curve for the $Ti_{12}V$ coincide with that of the pure Ti_{13} cluster, which has been calculated with the *all-electron* method.[5] For $Ti_{12}V$ and its first neighbors, the V impurity LDOS is localized farther from the Fermi level, (at E= -2 eV from E_F), which explains the increase in stability for these clusters. However, except for the Ti_nV clusters studied in this work, the V impurity LDOS has a scarce contribution at the Fermi level. Since these clusters adopt the same structures than pure Ti_n, we expect that the reactivity properties are not significantly changed except for $Ti_{1-2}V$ clusters, in which a larger highest-lowest occupied molecular orbital (HOMO-LUMO) gap may reduce the reactivity of the clusters.[35] This results motivate us for investigating Ti_nV_m bimetallic clusters which may offer opportunities for tuning the electronic properties with an appropriate composition.

Recently, it was found that Ti-based nanomaterials have a high-capacity hydrogen storage.[36–39] The chemical reactivity of small Ti_n clusters towards dissociative chemisorption of H_2 has been documented recently.[5] These works suggest that the chemisorption of one H_2 molecule has size dependent behaviour, with Ti_{13} being the most reactive cluster towards H_2 chemisorption. According to our present findings, we suggest that $Ti_{12}M$ clusters which favor the encapsulation of the M-dopant atom (e.g., M=B, Al and presently V) are promising, since titanium (the active site) remains on the surface. We are currently exploring the reactivity and electronic properties of the $Ti_{12}M$ clusters when they are modified by differ-

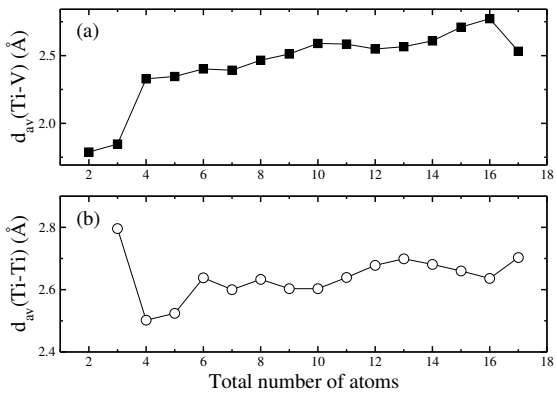

Figure 4: The Ti-V (a) and Ti-Ti (b) average binding distance of the most stable Ti_nV clusters is presented.

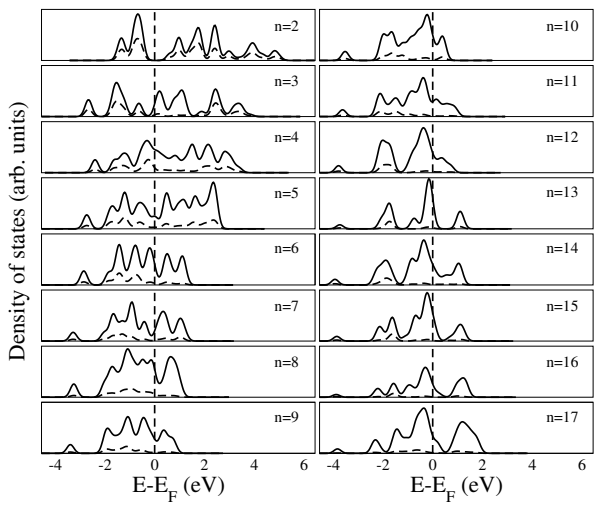

Figure 5: The total DOS of $Ti_{n-1}V$ clusters (solid curve) and LDOS of the V atom (dashed curve) is presented. A Gaussian broadening of 0.2 eV is used. The Fermi level is set at zero energy, denoted by a vertical dashed line.

ent impurity elements, with the belief to identify novel potential applications of M-doped Ti clusters.

Conclusions

In this work, the electronic and geometric structures of Ti_n and Ti_nV ($n = 1-16$) have been investigated using density functional theory (DFT) calculations with the generalized gradient

approximation (GGA). The lowest-energy structures of Ti_nV cluster have been determined by extensive searches for each cluster size. In the ground state structures of the Ti_nV clusters, the V atom prefers to occupy the surface site when $n \leqslant 8$ and $n = 16$, while for $n = 9$ up to 15, the V impurity falls in the center of the cage. Maximum peaks are observed for Ti_nV clusters at $n = 6$, 12 and 14 on the second-order energy difference, due to a relatively higher stability. We also found that when a single V impurity is added on Ti_n clusters an increase in the average binding energy occurs especially for $n = 12$, suggesting that the $Ti_{12}V$ cluster favors the encapsulation of the V-dopant atom. We are also currently exploring the reactivity and electronic properties of the $Ti_{12}M$ clusters when they are modified by different impurity elements, with the belief to identify novel potential applications of M-doped Ti clusters. Additionally, the electronic structures of small Ti_nV ($n \leqslant 4$) clusters exhibit a transition from metallic-like to semi-metallic electronic structure, while for $n = 5$ onwards, no significant changes are observed compared to pure Ti_n clusters. This results motivate us to investigate Ti_nV_m bimetallic clusters which may offer opportunities for tuning the electronic properties for appropriate and specific purposes.

Acknowledgement

The authors would like to acknowledge high-performance computing support from J. C. Sánchez-Leanos of Instituto de Física. First author thanks Computational Supercomputing Center CNS (San Luis Potosí, México) for providing computing resources.

References

(1) Bansmann, J.; Baker, S.; Binns, C.; Blackman, J.; Bucher, J.-P.; Dorantes-Dávila, J.; Dupuis, V.; Favre, L.; Kechrakos, D.; Kleibert, A. et al. Magnetic and Structural Properties of Isolated and Assembled Clusters. *Surf. Sci. Rep.* **2005**, *56*, 189 – 275.

(2) Khanna, S.; Castleman, A. *Quantum Phenomena in Clusters and Nanostructures*; Springer, 2014.

(3) Eustis, S.; El-Sayed, M. A. Why Gold Nanoparticles are more Precious than Pretty Gold: Noble Metal Surface Plasmon Resonance and its Enhancement of the Radiative and Nonradiative Properties of Nanocrystals of Different Shapes. *Chem. Soc. Rev.* **2006**, *35*, 209–217.

(4) Grande-Aztatzi, R.; Martínez-Alanis, P. R.; Cabellos, J. L.; Osorio, E.; Martínez, A.; Merino, G. Structural Evolution of Small Gold Clusters doped by One and Two Boron Atoms. *J. Comput. Chem.* **2014**, *35*, 2288–2296.

(5) Dhilip Kumar, T. J.; Weck, P. F.; Balakrishnan, N. Evolution of Small Ti Clusters and the Dissociative Chemisorption of H_2 on Ti. *J. Phys. Chem. C* **2007**, *111*, 7494–7500.

(6) Kant, A.; Lin, S. Dissociation Energies of Ti_2 and V_2. *J. Chem. Phys.* **1969**, *51*, 1644–1647.

(7) Haslett, T.; Moskovits, M.; Weitzman, A. Dissociation Energies of Transition Metal Diatomics. *J. Mol. Spectrosc.* **1989**, *135*, 259–269.

(8) Doverstål, M.; Lindgren, B.; Sassenberg, U.; Arrington, C. A.; Morse, M. D. The $^3\Pi_{0u} \leftarrow X^3\Delta_{1g}$ Band System of Jetcooled Ti_2. *J. Chem. Phys.* **1992**, *97*, 7087–7092.

(9) Russon, L. M.; Heidecke, S. A.; Birke, M. K.; Conceicao, J.; Morse, M. D.; Armentrout, P. B. Photodissociation Measurements of Bond Dissociation Energies: Ti^{+2}, V^{+2}, Co^{+2}, and Co^{+3}. *J. Chem. Phys.* **1994**, *100*, 4747–4755.

(10) Cossé, C.; Fouassier, M.; Mejean, T.; Tranquille, M.; DiLella, D. P.; Moskovits, M. Dititanium and Divanadium. *J. Chem. Phys.* **1980**, *73*, 6076–6085.

(11) Sakurai, M.; Watanabe, K.; Sumiyama, K.; Suzuki, K. Magic Numbers in Transition

Metal (Fe, Ti, Zr, Nb, and Ta) Clusters Observed by Time-of-flight Mass Spectrometry. *J. Chem. Phys.* **1999**, *111*, 235–238.

(12) Wu, H.; Desai, S. R.; Wang, L.-S. Electronic Structure of small Titanium Clusters: Emergence and Evolution of the 3*d* Band. *Phys. Rev. Lett.* **1996**, *76*, 212–215.

(13) Wei, S. H.; Zeng, Z.; You, J. Q.; Yan, X. H.; Gong, X. G. A Density-Functional Study of Small Titanium Clusters. *J. Chem. Phys.* **2000**, *113*, 11127–11133.

(14) Zhao, J.; Qiu, Q.; Wang, B.; Wang, J.; Wang, G. Geometric and Electronic Properties of Titanium Clusters Studied by Ultrasoft Pseudopotential. *Solid State Commun.* **2001**, *118*, 157 – 161.

(15) Salazar-Villanueva, M.; Hernández Tejeda, P. H.; Pal, U.; Rivas-Silva, J. F.; Rodríguez Mora, J. I.; Ascencio, J. A. Stable Ti_n ($n = 215$) Clusters and Their Geometries: DFT Calculations. *J. Phys. Chem. A* **2006**, *110*, 10274–10278.

(16) de Heer, W. A. The Physics of Simple Metal Clusters: Experimental Aspects and Simple Models. *Rev. Mod. Phys.* **1993**, *65*, 611–676.

(17) Xiang, J.; Wei, S. H.; Yan, X. H.; You, J. Q.; Mao, Y. L. A Density-Functional Study of Al-doped Ti Clusters: Ti_nAl ($n = 1 - 13$). *J. Chem. Phys.* **2004**, *120*, 4251–4257.

(18) Du, J.; Sun, X.; Chen, J.; Jiang, G. The Changes in the Geometrical, Electronic and Magnetic Properties of Titanium Clusters as one Titanium Atom is Substituted by Boron. *J. Phys. B* **2010**, *43*, 205103.

(19) Du, J. G.; Sun, X. Y.; Jiang, G. A DFT Study on small M-doped Titanium (M = V, Fe, Ni) Clusters: Structures, Chemical Bonds and Magnetic Properties. *Eur. Phys. J. D* **2009**, *55*, 111–120.

(20) Goedecker, S.; Hellmann, W.; Lenosky, T. Global Minimum Determination of the Born-Oppenheimer Surface within Density Functional Theory. *Phys. Rev. Lett.* **2005**, *95*, 055501.

(21) Zhang, M.; Fournier, R. Density-Functional-Theory Study of 13-Atom Metal Clusters. *Phys. Rev. A* **2009**, *79*, 043203.

(22) Rodríguez-Kessler, P. L.; Rodríguez-Domínguez, A. R. Size and Structure Effects of Pt_N ($N = 12 - 13$) Clusters for the Oxygen Reduction Reaction: First-Principles Calculations. *J. Chem. Phys.* **2015**, *143*, 12378–12384.

(23) Hohenberg, P.; Kohn, W. Inhomogeneous Electron Gas. *Phys. Rev.* **1964**, *136*, B864–B871.

(24) Kohn, W.; Sham, L. J. Self-Consistent Equations Including Exchange and Correlation Effects. *Phys. Rev.* **1965**, *140*, A1133–A1138.

(25) Kresse, G.; Hafner, J. *Ab initio* Molecular Dynamics for Liquid Metals. *Phys. Rev. B* **1993**, *47*, 558–561.

(26) Kresse, G.; Furthmüller, J. Efficient Iterative Schemes for *Ab initio* Total-Energy Calculations using a Plane-Wave Basis Set. *Phys. Rev. B* **1996**, *54*, 11169–11186.

(27) Blöchl, P. E. Projector Augmented-Wave Method. *Phys. Rev. B* **1994**, *50*, 17953–17979.

(28) Perdew, J. P.; Burke, K.; Ernzerhof, M. Generalized Gradient Approximation Made Simple. *Phys. Rev. Lett.* **1997**, *78*, 1396–1396.

(29) Makov, G.; Payne, M. C. Periodic Boundary Conditions in *Ab initio* Calculations. *Phys. Rev. B* **1995**, *51*, 4014–4022.

(30) Venkataramanan, N. S.; Sahara, R.; Mizuseki, H.; Kawazoe, Y. Titanium-Doped Nickel Clusters $TiNi_n$ ($n = 1-12$): Geometry, Electronic, Magnetic, and Hydrogen Adsorption Properties. *J. Phys. Chem. A* **2010**, *114*, 5049–5057.

(31) Doverstål, M.; Karlsson, L.; Lindgren, B.; Sassenberg, U. The $^3\Delta_u - X^3\Delta_g$ Band System of Jet-Cooled Ti_2. *Chem. Phys. Lett.* **1997**, *270*, 273 – 277.

(32) Tzeli, D.; Mavridis, A. Electronic Structure and Bonding of the 3d Transition Metal Borides, MB, M=Sc, Ti, V, Cr, Mn, Fe, Co, Ni, and Cu through all Electron Ab initio Calculations. *J. Chem. Phys.* **2008**, *128*, 034309.

(33) Anderson, A. B. Structures, Binding energies, and Charge Distributions for Two to Six atom Ti, Cr, Fe, and Ni Clusters and Their Relationship to Nucleation and Cluster Catalysis. *J. Chem. Phys.* **1976**, 4046–4055.

(34) Liu, S.-R.; Zhai, H.-J.; Castro, M.; Wang, L.-S. Photoelectron Spectroscopy of Ti_n Clusters ($n = 1 - 130$). *J. Chem. Phys.* **2003**, *118*, 2108–2115.

(35) Jimenez-Izal, E.; Moreno, D.; Mercero, J. M.; Matxain, J. M.; Audiffred, M.; Merino, G.; Ugalde, J. M. Doped Aluminum Cluster Anions: Size Matters. *J. Phys. Chem. A* **2014**, *118*, 4309–4314.

(36) Wang, J.; Ebner, A. D.; Ritter, J. A. Kinetic Behavior of Ti-Doped NaAlH4 When Cocatalyzed with Carbon Nanostructures. *J. Phys. Chem. B* **2006**, *110*, 17353–17358.

(37) Akman, N.; Durgun, E.; Yildirim, T.; Ciraci, S. Hydrogen Storage Capacity of Titanium Met-cars. *J. Phys. Condens. Matt.* **2006**, *18*, 9509.

(38) Yildirim, T.; Ciraci, S. Titanium-Decorated Carbon Nanotubes as a Potential High-Capacity Hydrogen Storage Medium. *Phys. Rev. Lett.* **2005**, *94*, 175501.

(39) Li, F.; Zhao, J.; Chen, Z. Hydrogen Storage Behavior of One-Dimensional TiB x Chains. *Nanotechnology* **2010**, *21*, 134006.

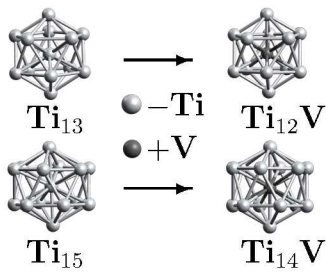
Ti13
−Ti
Ti12V
+V
Ti15
Ti14V